

Partial Covering Interpretation of the X-Ray Spectrum of the NLS1 1H 0707–495

Yasuo TANAKA, Thomas BOLLER, Luigi GALLO & Ralph KEIL

Max-Planck-Institut für Extraterrestrische Physik, Giessenbachstraße, 85748 Garching, Germany
and

Yoshihiro UEDA

Institute of Space and Astronautical Science, 3-1-1 Yoshinodai, Sagamihara, Kanagawa 229, Japan

(Received 2004 March 10; accepted 2004 April 9)

Abstract

The X-ray spectrum of 1H 0707–495 obtained with XMM-Newton showing a deep flux drop at ~ 7 keV (Boller et al. 2002) is studied based on the partial covering concept. The previously inferred extreme iron overabundance can be reduced down to $\sim 3\times$ solar if the hard component gradually steepens at high energies. The spectral shape supports that 1H 0707–495 is an AGN analogue of the galactic black-hole binaries in the soft state. Interpreting the soft excess as the emission from an optically-thick disk, the minimum black hole mass M is estimated to be $2 \cdot 10^6 M_{\odot}$ from the intrinsic luminosity corrected for partial covering. Based on the slim disk model, the observed disk temperature implies that the luminosity is close to the Eddington limit. The rapid and large flux variations with little change in the spectral shape can also be explained, if not all, as due to changes in the partial covering fraction. Partial covering may account for the large variability characteristics of NLS1.

Key words: galaxies: active – galaxies: individual: 1H 0707–495 – galaxies: Seyfert – X-rays: galaxies

1. Introduction

The X-ray spectrum of the narrow-line Seyfert 1 galaxy (NLS1) 1H 0707–495 ($z = 0.0411$) observed with XMM-Newton revealed a pronounced flux drop by a factor of $\gtrsim 3$ at ~ 7 keV (Boller et al. 2002, hereafter referred to as Paper 1). The measured edge energy and its sharpness suggest K-absorption by essentially neutral iron. However, there is no detectable fluorescence line at 6.4 keV (rest frame). In contrast to the strong iron K-absorption, the soft excess dominating below ~ 1 keV is little absorbed.

Two possibilities for these distinct features were discussed in Paper 1, i.e. (1) partial

covering and (2) reflection from an ionized disk. Both models require an extreme iron overabundance for the large depth of the edge ($\sim 35\times$ solar for partial covering of a power law model). The disk reflection model has been elaborated on by Fabian et al. (2002), considering reflections on sheets of dense material presumably formed by disk instabilities. Their model can account for the observed spectral features with an iron abundance of $\sim 5\times$ solar.

In this paper, we pursue the partial covering concept. The observed spectral features (little low-energy absorption, deep iron K-edge, and the absence of a prominent fluorescence line) are consistent with a partial covering phenomenon. In fact, similar features were observed in galactic X-ray binaries, and explained as due to partial covering (Brandt et al. 1996; Tanaka et al. 2003).

The spectral shape of 1H 0707–495 (an intense soft component and a hard tail) is similar to those of the galactic black-hole binaries in the soft state at high-luminosities (Tanaka, Shibazaki 1996), except that the soft excess lies in a much lower energy range. We consider that the soft excess of 1H 0707–495 is the emission from an optically-thick accretion disk as in the case of the soft-state black-hole binaries, and analyze the spectrum based on the partial covering concept with particular attention to the iron overabundance problem.

It should be mentioned that the model described in this paper has also been applied to the analysis of the XMM-Newton data of another NLS1 IRAS 13224–3809 (Boller et al. 2003) which showed a similar spectral shape and a deep flux drop as observed in 1H 0707–495.

Using the results of the analysis, we try to constrain the central black hole mass of 1H 0707–495. A possibility that the fast X-ray variability is due to changing covering fraction is also discussed.

2. Spectral Analysis

The XMM-Newton observation of 1H 0707–495 and the data processing are described in Paper 1. The X-ray spectrum shown in Paper 1 is used for the present analysis.

The observed spectrum of the soft excess is well reproduced by the multi-color blackbody disk (MCD) model (Mitsuda et al. 1984; Makishima et al. 2000) that approximates the spectrum of an optically-thick disk. A single-temperature blackbody model also gives an equally good fit, which is expected since the downward slope of MCD has a blackbody shape.

2.1. Low-Energy Absorption

First, we determine the low-energy absorption from the data in the 0.3–2 keV range. Simultaneous fitting is performed on all of the EPIC (MOS1, MOS2, and pn) spectra, utilizing a model consisting of a MCD or a blackbody and a power-law, modified by absorption. The parameter values for all three spectra are kept the same except for the normalization.

Simple absorption by neutral gas of cosmic abundances is found to be inadequate. An acceptable fit is obtained if an absorption edge is added at ~ 0.37 keV. This may be the K-edge

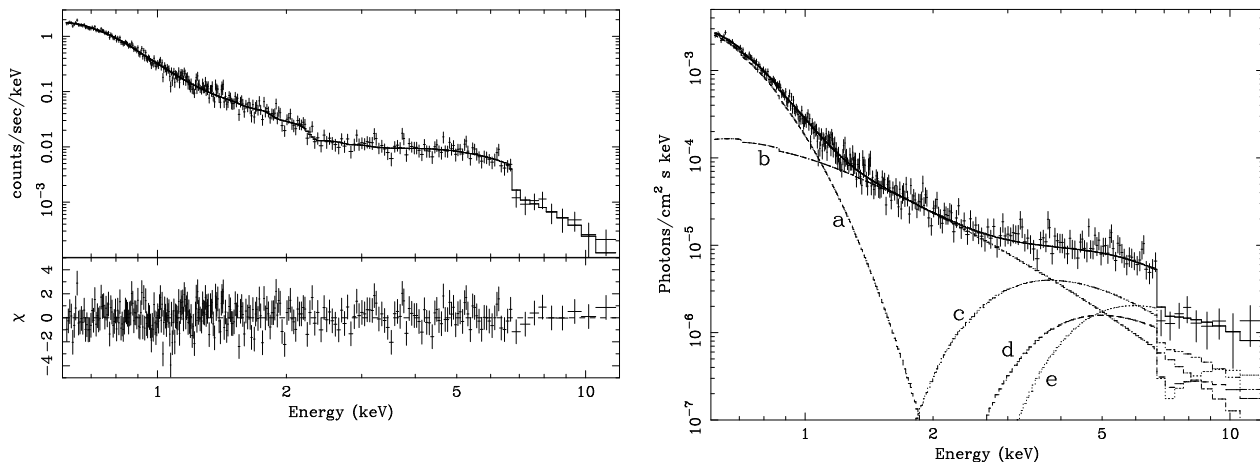


Fig. 1. Double partial covering applied to the model consisting of a MCD and a cut-off power law. The left panel is the best fit (Fe abundance $13\times$ solar) to the observed spectrum, and the right panel is the unfolded spectrum showing the model components: (a) the MCD and (b) the cut-off power law. (c), (d) and (e) are those absorbed with column densities N_{H} , $N_{\text{H},2}$, and $N_{\text{H}} + N_{\text{H},2}$, respectively (see Formula (2)).

of C V (0.39 keV, rest frame) of a warm absorber. For a MCD model, we obtain an absorption column of $\sim 1.3 \times 10^{21} \text{ cm}^{-2}$ including the interstellar absorption, and the depth of the 0.37-keV edge $\tau \sim 1.3$. A blackbody model gives slightly less absorption, $\sim 1.1 \times 10^{21} \text{ cm}^{-2}$ and $\tau \sim 1.2$. Note that these values are still subject to calibration uncertainties in the low-energy region. The best-fit MCD temperature (the highest color temperature of the disk) is $kT_{\text{in}} \sim 100 \text{ eV}$, and $kT_{\text{bb}} \sim 92 \text{ eV}$ for the blackbody temperature. The power-law photon index Γ is ~ 2.4 for both models. For the later analysis we fix these absorption parameters.

2.2. Partial Covering Spectral Analysis

We analyze the spectrum over the range 0.6–12 keV. We use only the pn data for its high detection efficiency at high energies. Exclusion of the data below 0.6 keV does not influence the fitting of the soft excess when the absorption parameters are fixed as determined above.

We employ the partial covering model with a neutral absorber as indicated by the observed energy of the iron K-edge. When a single absorber is responsible for partial covering, the fitting model is expressed as

$$[fe^{-\sigma N_{\text{H}}} + (1 - f)][F_{\text{soft}}(E) + F_{\text{hard}}(E)] , \quad (1)$$

where f denotes the covering fraction by an absorber of a column density N_{H} , and σ the photoabsorption cross section containing the Fe abundance as a free parameter. $F_{\text{soft}}(E)$ and $F_{\text{hard}}(E)$ are the model functions of the soft and hard components, respectively.

If a straight power law is employed for $F_{\text{hard}}(E)$, an extreme Fe abundance ($\sim 50\times$ solar) is required. The situation improves substantially if double partial covering by two separate absorbers is considered and expressed as

Table 1. Results of the fitting with the partial covering model.

Hard component	Fe abundance	Γ	E_c	f	N_H	f_2	$N_{H,2}$	χ^2/ν
	\times solar		keV		10^{22} cm^{-2}		10^{22} cm^{-2}	
Power law	30 best fit	2.7	∞	0.39	0.7	0.84	4.6	301/293
	5	3.4	∞	0.66	1.8	0.90	17.5	304/294
Cut-off power law	26 best fit	2.2	9.2	0.85	5.1	–	–	301/294
	5	1.9	4.2	0.88	16.7	–	–	304/295
Cut-off power law	13 best fit	2.3	8.0	0.62	4.2	0.73	10.3	297/292
	5	2.2	4.5	0.71	7.8	0.76	22.7	298/293
	2.5	2.0	2.8	0.78	11.4	0.79	37.9	300/293

$$[fe^{-\sigma N_H} + (1-f)][f_2e^{-\sigma N_{H,2}} + (1-f_2)] \times [F_{\text{soft}}(E) + F_{\text{hard}}(E)] , \quad (2)$$

where f_2 is the covering fraction of the second absorber of a column density $N_{H,2}$. Double partial covering is also an approximation for the sum of two absorbed components with different column densities, as well as for more complex cases involving multiple absorbed components. Evidence for double partial covering was found in the spectrum of the X-ray binary GRO 1655–40 during a dip-like event (Tanaka et al. 2003).

A double partial covering gives a good fit for a power-law model in 1H 0707–495 with $\chi^2_{\text{min}}/\nu = 301/293$. The best-fit Fe abundance is as large as $30\times$ solar, similar to the result of Paper I. The acceptable range within 90% limit ($\chi^2_{\text{min}} + 2.71$) extends down to $5\times$ solar, although the power-law becomes very steep with a photon index $\Gamma \sim 3.4$ (see table 1).

We notice a general trend that Γ increases as the Fe abundance is reduced. This suggests that gradual steepening of the hard tail toward high energies would allow for lower Fe abundances. For such a spectral model, we employ a cut-off power law of the form $E^{-\Gamma}e^{-E/E_c}$.

First, when single partial covering [Formula (1)] is assumed, we find a shallow minimum around the best-fit Fe abundance of $26\times$ solar ($\chi^2_{\text{min}}/\nu = 301/294$). Fe abundance down to $5\times$ solar is acceptable at 90% limit (see table 1). The main difference from the simple power-law case is that the average Γ below ~ 5 keV stays at around ~ 2.5 over the wide range of Fe abundance.

Double partial covering [Formula (2)] with a cut-off power law model allows for even smaller Fe abundances. While the best-fit value is $\sim 13\times$ solar ($\chi^2_{\text{min}}/\nu = 300/292$), the 90%-confidence lower limit is $2.5\times$ solar (see table 1). The average Γ in the range 2–5 keV is also ~ 2.5 . The best spectral fit is shown in figure 1.

The parameter values obtained from these fits with a MCD soft component model are listed in table 1. A blackbody model gives essentially the same results. Differences in the hard component model do not affect the fits of the soft component because the latter dominates the observed spectrum. The absorption-corrected soft component accounts for $\sim 90\%$ of the total flux above 0.3 keV. On the other hand, the intrinsic flux (corrected for covering) depends on the covering model (single or double) and the Fe abundance, which cause differences in the covering fraction (see table 1).

3. Discussion

The observed spectral shape of 1H 0707–495 showing an intense soft component and a hard tail is strikingly similar to those of the black-hole binaries in the soft state. The soft component which displays a blackbody-shaped spectrum and lack of prominent line features is consistent with the emission from an optically-thick disk. The hard component shows an average photon index $\Gamma \sim 2.5$, similar to the hard tail of the black-hole binaries in the soft state, and distinctly softer than in the hard state ($\Gamma \sim 1.8$).

These properties are fairly common among NLS1 (e.g. Boller 2000), suggesting that they are AGN analogues of the soft-state black-hole binaries. This was first pointed out for the NLS1 RE 1034+39 by Pounds et al. (1995). In contrast, most other AGNs show harder power-law spectra, analogous to the black-hole binaries in the hard state at low luminosities.

3.1. *Partial Covering and Iron Abundance*

The observed spectral features (little low-energy absorption and deep Fe K-absorption without a prominent fluorescence line) are typical of partial covering. That is, the central source is covered by absorbing clouds in the line of sight; however, either the absorber is patchy so that a fraction of the emission leaks through, or the photons which are electron-scattered off the source form the unabsorbed component.

Table 1 shows that the covering fraction is roughly 90%, i.e. the intrinsic source flux is an order of magnitude higher than the observed time-averaged flux (corresponding to the spectrum analyzed here). This is not surprisingly high, considering that the peak flux during this observation was ~ 3 times the average (see figure 3 of Paper 1).

In Paper 1 an excessively large ($\sim 30\times$ solar) Fe abundance was required for partial covering of a power-law model. However, the present analysis shows that the Fe abundance depends on the shape of the hard continuum, which is still uncertain. Gradual steepening of the hard component (modelled with a cut-off power law) allows for lower Fe abundances. Double partial covering gives the lowest acceptable Fe abundance of $2.5\times$ solar, which is still suggestive of substantial overabundance. Accurate determination requires much better statistics above the edge to constrain the shape of the hard component.

A similarly deep flux drop was discovered from IRAS 13224–3809, also attributable to

the Fe-K edge (Boller et al. 2003). The same partial covering model as used here also gives an Fe overabundance of $\sim 10\times$ solar (the 90% confidence lower limit being $2\times$ solar) and requires a large covering fraction of $\gtrsim 80\%$ (see Boller et al. 2003 for detail).

Such a deep flux drop (by a factor of > 3) has rarely been observed. Whether or not these two sources are exceptional among NLS1 is an interesting question. In this respect, it is to be noticed that the depth of the edge changes with the covering fraction, i.e., the larger the covering fraction, the deeper the edge becomes (see figure 2 in subsection 3.3). Therefore, in addition to the effect of Fe overabundance, the edges of these two NLS1 might be deepened due to particularly large covering fraction compared to other NLS1 observed. Thus, the question still remains open at present. (Note that the covering fraction may change with time.)

3.2. Mass of the Central Object and Accretion Rate

We try to constrain the mass of the central object in 1H 0707–495 from the bolometric luminosity L_{bol} and the innermost disk (color) temperature T_{in} . For estimating L_{bol} , the MCD model is valid only for $L_{\text{bol}} \ll L_{\text{E}}$, where L_{E} is the Eddington luminosity. As L_{bol} approaches L_{E} (which is the case as shown below), the spectral energy distribution deviates from the MCD model due to enhanced Comptonization in the innermost disk (e.g. Ross et al. 1992); thus the MCD model overestimates L_{bol} . We evaluate here the minimum value of L_{bol} by employing the present result for a single blackbody model instead of a MCD model.

For the Fe abundance range of $(2.5 - 5)\times$ solar, the bolometric blackbody flux corrected for covering (according to table 1) is in the range $(1.0 - 1.5) \cdot 10^{-10} \text{ erg cm}^{-2}\text{s}^{-1}$ (excluding the steep power-law case of $\Gamma = 3.4$, see table 1). Furthermore, we consider a face-on disk for estimating a minimum bolometric luminosity L_{min} . Thus-obtained L_{min} is $\sim (2 - 3) \cdot 10^{44} \text{ erg s}^{-1}$ for $z = 0.0411$ and $H_0 = 70 \text{ km s}^{-1}\text{Mpc}^{-1}$. Assuming $L_{\text{min}} < L_{\text{E}}$, the minimum mass of the central object M_{min} is around $2 \cdot 10^6 M_{\odot}$.

On the other hand, the observed disk temperature (100 eV for a MCD and 92 eV for a blackbody) is very high for a standard disk around a Schwarzschild hole of such a mass. If the MCD model is used, adopting a color correction factor ($T_{\text{in}}/T_{\text{eff}}$) of 2.4 (Ross et al. 1992), the observed temperature exceeds the limit ($\sim 80 \text{ eV}$) at $L_{\text{bol}} = L_{\text{E}}$ [from equation (12) of Makishima et al. 2000]. Although the result from the MCD model may no longer be accurate near L_{E} , it clearly indicates an extremely high accretion rate.

A slim disk model, first proposed by Abramowicz et al. (1988), applies at such high accretion rates as $\dot{M} \gg L_{\text{bol}}/c^2$. In this case, significant radiation can come from within 3 Schwarzschild radii, hence T_{in} may exceed the limit of a standard thin disk. Detailed spectral properties of a slim disk have been studied (e.g. Mineshige et al. 2000; Watarai et al. 2001).

Based on this slim disk model, we extrapolate figure 1 of Watarai et al. (2001), which displays the $L_{\text{bol}} - T_{\text{in}}$ relation for different M -values of a Schwarzschild hole, and obtain the minimum mass $M_{\text{min}} \sim 2 \cdot 10^6 M_{\odot}$ and $L_{\text{min}} \approx L_{\text{E}}$ which corresponds to $\dot{M} \sim 16(L/c^2)$. Considering

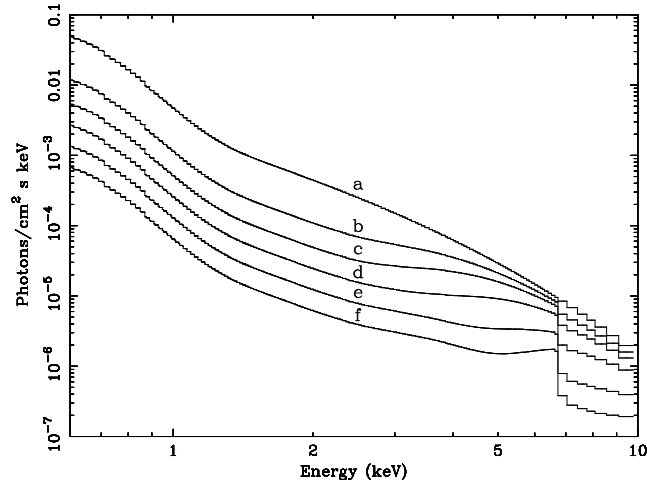


Fig. 2. Spectra expected from double partial covering of a MCD + a cut-off power law model for different f_2 and $N_{\text{H},2}$. (a) is the intrinsic spectrum ($f = f_2 = 0$), and (b)–(f) are for the sets of $(f_2, N_{\text{H},2}$ in units of 10^{22} cm^{-2}) $(0, 0)$, $(0.56, 16)$, $(0.78, 33)$, $(0.89, 60)$ and $(0.94, 90)$, respectively.

that true $L_{\text{bol}} > L_{\text{min}}$, M will be a little larger than $2 \cdot 10^6 M_{\odot}$, and then L_{bol} will slightly exceeds L_{E} for the observed disk temperature.

3.3. Time Variability

As discussed above, the X-ray spectrum of 1H 0707–495 is characteristic of the soft state. However, it displays extreme variability on time scales as short as 10^3 s. This is distinctly different from the black-hole X-ray binaries in the soft state in which the variability is relatively small. (Tanaka, Shibazaki 1996). Importantly, as reported in Paper 1, 1H 0707–495 shows insignificant spectral variability during the large flux variations of more than a factor of 4. For an optically-thick disk to change luminosity this much, the disk temperature T_{in} must change quite significantly, $\gtrsim 40\%$, which is not observed. The same holds true for another highly-variable NLS1 IRAS 13224–3809 which showed even larger flux variations than 1H 0707–495 without changing T_{in} (Boller et al. 2003; Gallo et al. 2004). We therefore suspect that the observed flux variations are not all due to the luminosity changes of the central source.

The possibility of partial covering causing large flux changes in NLS1 was previously considered (Boller et al. 1997; Brandt & Gallagher 2000). Tanaka et al. (2003) demonstrated, from a study of a dip in the light curve of GRO J1655-40, that spectrum-invariant flux changes can occur as a result of changes in partial covering conditions. A similar condition is illustrated in figure 2 for the case of 1H 0707–495. The parameters of the MCD and of one partial coverer (f and N_{H}) are fixed to the best-fit values of the observed spectrum (Fe abundance of $3 \times$ solar assumed), and those of the second coverer (f_2 and $N_{\text{H},2}$) are varied. Among them, (a) is the intrinsic spectrum and (d) is the best fit to the observed spectrum. The spectral shapes of (b) through (f) are similar to each other over a flux range of an order of magnitude. Positive correlation between f_2 and $N_{\text{H},2}$ is plausible, as discussed in Tanaka et al. (2003).

The observed light curve of 1H 0707–495 (figure 3 of Paper 1) appears as consisting of random “flares” of various peak fluxes, each lasting typically $\sim 3 \cdot 10^3$ s. Such flux changes can be explained qualitatively as follows: If the azimuthal distribution of the covering clouds is non-uniform, the covering fraction varies according to the orbital motion of the clouds. A local minimum of the covering fraction corresponds to a flare peak.

The duration of a flare is the time that a local minimum of covering takes to scan the electron-scattering region from a distance r at the Keplerian velocity $c(r_g/r)^{1/2}$, where r_g is the gravitational radius. Suppose the electron-scattering region has an extension of $\sim 10r_g$, then the observed time scale is understood when these clouds are located around $r \sim 400r_g$ ($\sim 2 \cdot 10^{14}$ cm) for $M \sim 3 \cdot 10^6 M_\odot$.

The essential neutrality of iron indicates low photoionization effect, i.e. the ionization parameter $\xi = L_h/nr^2 \lesssim 1$, where L_h is the hard component luminosity and n the atomic density. This requires that $n \gtrsim 10^{14} \text{ cm}^{-3}$ for an estimated $L_h \sim 10^{43} \text{ erg s}^{-1}$. Such dense clouds are probably confined by magnetic fields (Rees 1987). In fact, the results from magneto-hydrodynamical simulations that demonstrate highly inhomogeneous and clumpy accretion flow are consistent with this view (e.g. Kawaguchi et al. 2000).

The persistent variation of the observed flux of 1H 0707–495 may be related to very high, possibly super-Eddington, luminosity (see subsection 3.2). At these accretion rates, various disk instabilities might produce inhomogeneities in the vertical direction, causing time-variable partial covering. An alternative possibility is that partial covering clouds may be formed from a radiation-driven mass outflow.

Large-amplitude variability is generally characteristic of NLS1. It is worth examining the associated spectral variation of other NLS1. If T_{in} of the soft component does not change with flux, it is possible that the flux variation may, at least in part, be due to changes in partial covering. If it were the case, the intrinsic luminosity, hence the black hole mass, could be significantly higher than estimated from the observed flux.

The authors are grateful to S. Mineshige for valuable comments.

References

- Abramowicz, M.A., Czerny, B., Lasota, J.P., & Szuszkiewicz, E. 1988, ApJ 332, 646
 Boller, Th., Brandt, W.N., Fabian, A.C., & Fink, H.H. 1997, MNRAS 289, 393
 Boller, Th. 2000, New Astron. Rev. 44, 387
 Boller, Th., et al. 2002, MNRAS 329, L1 (Paper 1)
 Boller, Th., Tanaka, Y., Fabian, A., Brandt, W.N., Gallo, L., Anabuki, N., Haba, Y., & Vaughan, S. 2003, MNRAS 343, L89
 Brandt, W.N., Fabian, A.C., Dotani, T., Nagase, F., Inoue, H., Kotani, T., & Segawa, Y. 1996, MNRAS 283, 1071

Brandt, W.N., Gallagher, & S.C. 2000, *New Astron. Rev.* 44, 461
Fabian, A.C., Ballantyne, D.R., Merloni, A., Vaughan, S., Iwasawa, K., & Boller, Th. 2002, *MNRAS* 331, L35
Gallo, L., Boller, Th., Tanaka, Y., Fabian, A.C., Brandt, W.N., Welsh, W. F., Anabuki, N. & Haba, Y. 2004, *MNRAS* 347, 269
Kawaguchi, T., Mineshige, S., Machida, M., Matsumoto, R., & Shibata, K. 2000, *PASJ* 52, L1
Makishima, K., et al. 2000, *ApJ* 535, 632
Mineshige, S., Kawaguchi, T., Takeuchi, M., & Hayashida, K. 2000, *PASJ* 52, 499
Mitsuda, K., et al. 1984, *PASJ* 36, 741
Pounds, K., Done, K., & Osborne, J.P. 1995, *MNRAS* 277, L5
Rees, M.J. 1987, *MNRAS* 228, 47p
Ross, R.R., Fabian, A.C., & Mineshige, S. 1992, *MNRAS* 258, 189
Tanaka, Y., & Shibazaki, N. 1996, *ARA&A* 34, 607
Tanaka, Y., Ueda, Y., & Boller, Th. 2003, *MNRAS* 338, L1
Watarai, K., Mizuno, T., & Mineshige, S. 2001, *ApJ* 549, L77

Partial Covering Interpretation of the X-Ray Spectrum of the NLS1 1H 0707–495

Yasuo TANAKA, Thomas BOLLER, Luigi GALLO & Ralph KEIL

Max-Planck-Institut für Extraterrestrische Physik, Giessenbachstraße, 85748 Garching, Germany
and

Yoshihiro UEDA

Institute of Space and Astronautical Science, 3-1-1 Yoshinodai, Sagami-hara, Kanagawa 229, Japan

(Received 2004 March 10; accepted 2004 April 9)

Abstract

The X-ray spectrum of 1H 0707–495 obtained with XMM-Newton showing a deep flux drop at ~ 7 keV (Boller et al. 2002) is studied based on the partial covering concept. The previously inferred extreme iron overabundance can be reduced down to $\sim 3 \times$ solar if the hard component gradually steepens at high energies. The spectral shape supports that 1H 0707–495 is an AGN analogue of the galactic black-hole binaries in the soft state. Interpreting the soft excess as the emission from an optically-thick disk, the minimum black hole mass M is estimated to be $2 \cdot 10^6 M_{\odot}$ from the intrinsic luminosity corrected for partial covering. Based on the slim disk model, the observed disk temperature implies that the luminosity is close to the Eddington limit. The rapid and large flux variations with little change in the spectral shape can also be explained, if not all, as due to changes in the partial covering fraction. Partial covering may account for the large variability characteristics of NLS1.

Key words: galaxies: active – galaxies: individual: 1H 0707–495 – galaxies: Seyfert – X-rays: galaxies

1. Introduction

The X-ray spectrum of the narrow-line Seyfert 1 galaxy (NLS1) 1H 0707–495 ($z = 0.0411$) observed with XMM-Newton revealed a pronounced flux drop by a factor of $\gtrsim 3$ at ~ 7 keV (Boller et al. 2002, hereafter referred to as Paper 1). The measured edge energy and its sharpness suggest K-absorption by essentially neutral iron. However, there is no detectable fluorescence line at 6.4 keV (rest frame). In contrast to the strong iron K-absorption, the soft excess dominating below ~ 1 keV is little absorbed.

Two possibilities for these distinct features were discussed in Paper 1, i.e. (1) partial

covering and (2) reflection from an ionized disk. Both models require an extreme iron overabundance for the large depth of the edge ($\sim 35\times$ solar for partial covering of a power law model). The disk reflection model has been elaborated on by Fabian et al. (2002), considering reflections on sheets of dense material presumably formed by disk instabilities. Their model can account for the observed spectral features with an iron abundance of $\sim 5\times$ solar.

In this paper, we pursue the partial covering concept. The observed spectral features (little low-energy absorption, deep iron K-edge, and the absence of a prominent fluorescence line) are consistent with a partial covering phenomenon. In fact, similar features were observed in galactic X-ray binaries, and explained as due to partial covering (Brandt et al. 1996; Tanaka et al. 2003).

The spectral shape of 1H 0707–495 (an intense soft component and a hard tail) is similar to those of the galactic black-hole binaries in the soft state at high-luminosities (Tanaka, Shibazaki 1996), except that the soft excess lies in a much lower energy range. We consider that the soft excess of 1H 0707–495 is the emission from an optically-thick accretion disk as in the case of the soft-state black-hole binaries, and analyze the spectrum based on the partial covering concept with particular attention to the iron overabundance problem.

It should be mentioned that the model described in this paper has also been applied to the analysis of the XMM-Newton data of another NLS1 IRAS 13224–3809 (Boller et al. 2003) which showed a similar spectral shape and a deep flux drop as observed in 1H 0707–495.

Using the results of the analysis, we try to constrain the central black hole mass of 1H 0707–495. A possibility that the fast X-ray variability is due to changing covering fraction is also discussed.

2. Spectral Analysis

The XMM-Newton observation of 1H 0707–495 and the data processing are described in Paper 1. The X-ray spectrum shown in Paper 1 is used for the present analysis.

The observed spectrum of the soft excess is well reproduced by the multi-color blackbody disk (MCD) model (Mitsuda et al. 1984; Makishima et al. 2000) that approximates the spectrum of an optically-thick disk. A single-temperature blackbody model also gives an equally good fit, which is expected since the downward slope of MCD has a blackbody shape.

2.1. Low-Energy Absorption

First, we determine the low-energy absorption from the data in the 0.3–2 keV range. Simultaneous fitting is performed on all of the EPIC (MOS1, MOS2, and pn) spectra, utilizing a model consisting of a MCD or a blackbody and a power-law, modified by absorption. The parameter values for all three spectra are kept the same except for the normalization.

Simple absorption by neutral gas of cosmic abundances is found to be inadequate. An acceptable fit is obtained if an absorption edge is added at ~ 0.37 keV. This may be the K-edge

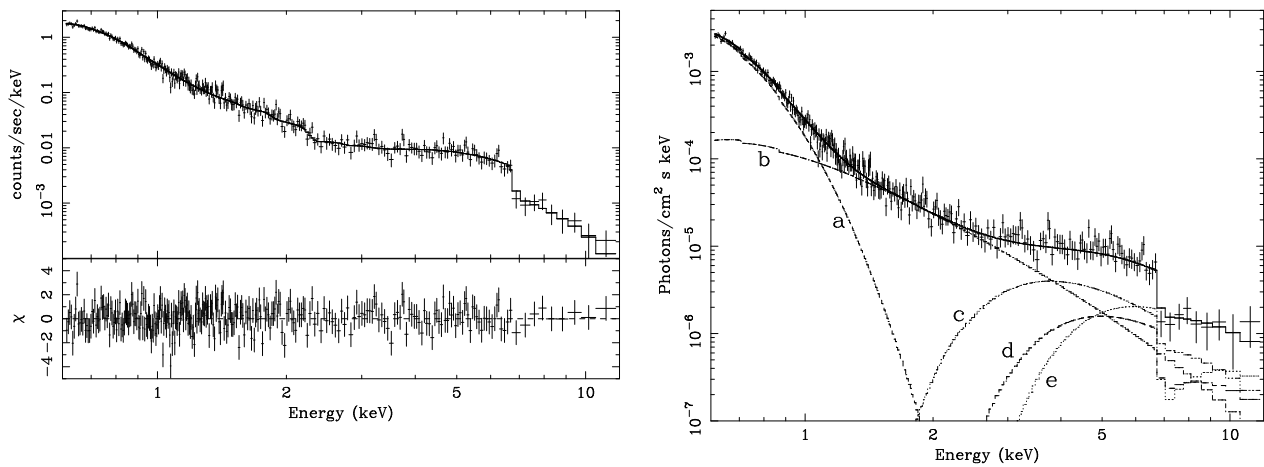


Fig. 1. Double partial covering applied to the model consisting of a MCD and a cut-off power law. The upper panel is the best fit (Fe abundance $13\times$ solar) to the observed spectrum, and the lower panel is the unfolded spectrum showing the model components: (a) the MCD and (b) the cut-off power law. (c), (d) and (e) are those absorbed with column densities N_{H} , $N_{\text{H},2}$, and $N_{\text{H}} + N_{\text{H},2}$, respectively (see Formula (2)).

of C V (0.39 keV, rest frame) of a warm absorber. For a MCD model, we obtain an absorption column of $\sim 1.3 \times 10^{21} \text{ cm}^{-2}$ including the interstellar absorption, and the depth of the 0.37-keV edge $\tau \sim 1.3$. A blackbody model gives slightly less absorption, $\sim 1.1 \times 10^{21} \text{ cm}^{-2}$ and $\tau \sim 1.2$. Note that these values are still subject to calibration uncertainties in the low-energy region. The best-fit MCD temperature (the highest color temperature of the disk) is $kT_{\text{in}} \sim 100 \text{ eV}$, and $kT_{\text{bb}} \sim 92 \text{ eV}$ for the blackbody temperature. The power-law photon index Γ is ~ 2.4 for both models. For the later analysis we fix these absorption parameters.

2.2. Partial Covering Spectral Analysis

We analyze the spectrum over the range 0.6–12 keV. We use only the pn data for its high detection efficiency at high energies. Exclusion of the data below 0.6 keV does not influence the fitting of the soft excess when the absorption parameters are fixed as determined above.

We employ the partial covering model with a neutral absorber as indicated by the observed energy of the iron K-edge. When a single absorber is responsible for partial covering, the fitting model is expressed as

$$[fe^{-\sigma N_{\text{H}}} + (1 - f)][F_{\text{soft}}(E) + F_{\text{hard}}(E)] , \quad (1)$$

where f denotes the covering fraction by an absorber of a column density N_{H} , and σ the photoabsorption cross section containing the Fe abundance as a free parameter. $F_{\text{soft}}(E)$ and $F_{\text{hard}}(E)$ are the model functions of the soft and hard components, respectively.

If a straight power law is employed for $F_{\text{hard}}(E)$, an extreme Fe abundance ($\sim 50\times$ solar) is required. The situation improves substantially if double partial covering by two separate absorbers is considered and expressed as

Table 1. Results of the fitting with the partial covering model.

Hard component	Fe abundance	Γ	E_c	f	N_H	f_2	$N_{H,2}$	χ^2/ν
	\times solar		keV		10^{22} cm $^{-2}$		10^{22} cm $^{-2}$	
Power law	30 best fit	2.7	∞	0.39	0.7	0.84	4.6	301/293
	5	3.4	∞	0.66	1.8	0.90	17.5	304/294
Cut-off power law	26 best fit	2.2	9.2	0.85	5.1	–	–	301/294
	5	1.9	4.2	0.88	16.7	–	–	304/295
Cut-off power law	13 best fit	2.3	8.0	0.62	4.2	0.73	10.3	297/292
	5	2.2	4.5	0.71	7.8	0.76	22.7	298/293
	2.5	2.0	2.8	0.78	11.4	0.79	37.9	300/293

$$[fe^{-\sigma N_H} + (1 - f)][f_2e^{-\sigma N_{H,2}} + (1 - f_2)] \times [F_{\text{soft}}(E) + F_{\text{hard}}(E)] , \quad (2)$$

where f_2 is the covering fraction of the second absorber of a column density $N_{H,2}$. Double partial covering is also an approximation for the sum of two absorbed components with different column densities, as well as for more complex cases involving multiple absorbed components. Evidence for double partial covering was found in the spectrum of the X-ray binary GRO 1655–40 during a dip-like event (Tanaka et al. 2003).

A double partial covering gives a good fit for a power-law model in 1H 0707–495 with $\chi^2_{\text{min}}/\nu = 301/293$. The best-fit Fe abundance is as large as $30\times$ solar, similar to the result of Paper I. The acceptable range within 90% limit ($\chi^2_{\text{min}} + 2.71$) extends down to $5\times$ solar, although the power-law becomes very steep with a photon index $\Gamma \sim 3.4$ (see table 1).

We notice a general trend that Γ increases as the Fe abundance is reduced. This suggests that gradual steepening of the hard tail toward high energies would allow for lower Fe abundances. For such a spectral model, we employ a cut-off power law of the form $E^{-\Gamma}e^{-E/E_c}$.

First, when single partial covering [Formula (1)] is assumed, we find a shallow minimum around the best-fit Fe abundance of $26\times$ solar ($\chi^2_{\text{min}}/\nu = 301/294$). Fe abundance down to $5\times$ solar is acceptable at 90% limit (see table 1). The main difference from the simple power-law case is that the average Γ below ~ 5 keV stays at around ~ 2.5 over the wide range of Fe abundance.

Double partial covering [Formula (2)] with a cut-off power law model allows for even smaller Fe abundances. While the best-fit value is $\sim 13\times$ solar ($\chi^2_{\text{min}}/\nu = 300/292$), the 90%-confidence lower limit is $2.5\times$ solar (see table 1). The average Γ in the range 2–5 keV is also ~ 2.5 . The best spectral fit is shown in figure 1.

The parameter values obtained from these fits with a MCD soft component model are listed in table 1. A blackbody model gives essentially the same results. Differences in the hard component model do not affect the fits of the soft component because the latter dominates the observed spectrum. The absorption-corrected soft component accounts for $\sim 90\%$ of the total flux above 0.3 keV. On the other hand, the intrinsic flux (corrected for covering) depends on the covering model (single or double) and the Fe abundance, which cause differences in the covering fraction (see table 1).

3. Discussion

The observed spectral shape of 1H 0707–495 showing an intense soft component and a hard tail is strikingly similar to those of the black-hole binaries in the soft state. The soft component which displays a blackbody-shaped spectrum and lack of prominent line features is consistent with the emission from an optically-thick disk. The hard component shows an average photon index $\Gamma \sim 2.5$, similar to the hard tail of the black-hole binaries in the soft state, and distinctly softer than in the hard state ($\Gamma \sim 1.8$).

These properties are fairly common among NLS1 (e.g. Boller 2000), suggesting that they are AGN analogues of the soft-state black-hole binaries. This was first pointed out for the NLS1 RE 1034+39 by Pounds et al. (1995). In contrast, most other AGNs show harder power-law spectra, analogous to the black-hole binaries in the hard state at low luminosities.

3.1. *Partial Covering and Iron Abundance*

The observed spectral features (little low-energy absorption and deep Fe K-absorption without a prominent fluorescence line) are typical of partial covering. That is, the central source is covered by absorbing clouds in the line of sight; however, either the absorber is patchy so that a fraction of the emission leaks through, or the photons which are electron-scattered off the source form the unabsorbed component.

Table 1 shows that the covering fraction is roughly 90%, i.e. the intrinsic source flux is an order of magnitude higher than the observed time-averaged flux (corresponding to the spectrum analyzed here). This is not surprisingly high, considering that the peak flux during this observation was ~ 3 times the average (see figure 3 of Paper 1).

In Paper 1 an excessively large ($\sim 30\times$ solar) Fe abundance was required for partial covering of a power-law model. However, the present analysis shows that the Fe abundance depends on the shape of the hard continuum, which is still uncertain. Gradual steepening of the hard component (modelled with a cut-off power law) allows for lower Fe abundances. Double partial covering gives the lowest acceptable Fe abundance of $2.5\times$ solar, which is still suggestive of substantial overabundance. Accurate determination requires much better statistics above the edge to constrain the shape of the hard component.

A similarly deep flux drop was discovered from IRAS 13224–3809, also attributable to

the Fe-K edge (Boller et al. 2003). The same partial covering model as used here also gives an Fe overabundance of $\sim 10\times$ solar (the 90% confidence lower limit being $2\times$ solar) and requires a large covering fraction of $\gtrsim 80\%$ (see Boller et al. 2003 for detail).

Such a deep flux drop (by a factor of > 3) has rarely been observed. Whether or not these two sources are exceptional among NLS1 is an interesting question. In this respect, it is to be noticed that the depth of the edge changes with the covering fraction, i.e., the larger the covering fraction, the deeper the edge becomes (see figure 2 in subsection 3.3). Therefore, in addition to the effect of Fe overabundance, the edges of these two NLS1 might be deepened due to particularly large covering fraction compared to other NLS1 observed. Thus, the question still remains open at present. (Note that the covering fraction may change with time.)

3.2. Mass of the Central Object and Accretion Rate

We try to constrain the mass of the central object in 1H 0707–495 from the bolometric luminosity L_{bol} and the innermost disk (color) temperature T_{in} . For estimating L_{bol} , the MCD model is valid only for $L_{\text{bol}} \ll L_{\text{E}}$, where L_{E} is the Eddington luminosity. As L_{bol} approaches L_{E} (which is the case as shown below), the spectral energy distribution deviates from the MCD model due to enhanced Comptonization in the innermost disk (e.g. Ross et al. 1992); thus the MCD model overestimates L_{bol} . We evaluate here the minimum value of L_{bol} by employing the present result for a single blackbody model instead of a MCD model.

For the Fe abundance range of $(2.5 - 5)\times$ solar, the bolometric blackbody flux corrected for covering (according to table 1) is in the range $(1.0 - 1.5) \cdot 10^{-10} \text{ erg cm}^{-2}\text{s}^{-1}$ (excluding the steep power-law case of $\Gamma = 3.4$, see table 1). Furthermore, we consider a face-on disk for estimating a minimum bolometric luminosity L_{min} . Thus-obtained L_{min} is $\sim (2 - 3) \cdot 10^{44} \text{ erg s}^{-1}$ for $z = 0.0411$ and $H_0 = 70 \text{ km s}^{-1}\text{Mpc}^{-1}$. Assuming $L_{\text{min}} < L_{\text{E}}$, the minimum mass of the central object M_{min} is around $2 \cdot 10^6 M_{\odot}$.

On the other hand, the observed disk temperature (100 eV for a MCD and 92 eV for a blackbody) is very high for a standard disk around a Schwarzschild hole of such a mass. If the MCD model is used, adopting a color correction factor ($T_{\text{in}}/T_{\text{eff}}$) of 2.4 (Ross et al. 1992), the observed temperature exceeds the limit ($\sim 80 \text{ eV}$) at $L_{\text{bol}} = L_{\text{E}}$ [from equation (12) of Makishima et al. 2000]. Although the result from the MCD model may no longer be accurate near L_{E} , it clearly indicates an extremely high accretion rate.

A slim disk model, first proposed by Abramowicz et al. (1988), applies at such high accretion rates as $\dot{M} \gg L_{\text{bol}}/c^2$. In this case, significant radiation can come from within 3 Schwarzschild radii, hence T_{in} may exceed the limit of a standard thin disk. Detailed spectral properties of a slim disk have been studied (e.g. Mineshige et al. 2000; Watarai et al. 2001).

Based on this slim disk model, we extrapolate figure 1 of Watarai et al. (2001), which displays the $L_{\text{bol}} - T_{\text{in}}$ relation for different M -values of a Schwarzschild hole, and obtain the minimum mass $M_{\text{min}} \sim 2 \cdot 10^6 M_{\odot}$ and $L_{\text{min}} \approx L_{\text{E}}$ which corresponds to $\dot{M} \sim 16(L/c^2)$. Considering

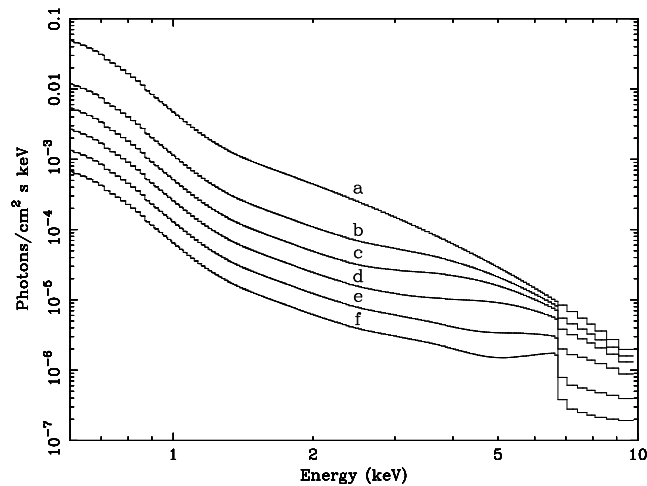


Fig. 2. Spectra expected from double partial covering of a MCD + a cut-off power law model for different f_2 and $N_{\text{H},2}$. (a) is the intrinsic spectrum ($f = f_2 = 0$), and (b)–(f) are for the sets of $(f_2, N_{\text{H},2}$ in units of 10^{22} cm^{-2}) (0, 0), (0.56, 16), (0.78, 33), (0.89, 60) and (0.94, 90), respectively.

that true $L_{\text{bol}} > L_{\text{min}}$, M can be a little larger than $2 \cdot 10^6 M_{\odot}$, and then L_{bol} somewhat exceeds L_{E} for the observed disk temperature.

3.3. Time Variability

As discussed above, the X-ray spectrum of 1H 0707–495 is characteristic of the soft state. However, it displays extreme variability on time scales as short as 10^3 s. This is distinctly different from the black-hole X-ray binaries in the soft state in which the variability is relatively small. (Tanaka, Shibazaki 1996). Importantly, as reported in Paper 1, 1H 0707–495 shows insignificant spectral variability during the large flux variations of more than a factor of 4. For an optically-thick disk to change luminosity this much, the disk temperature T_{in} must change quite significantly, $\gtrsim 40\%$, which is not observed. The same holds true for another highly-variable NLS1 IRAS 13224–3809 which showed even larger flux variations than 1H 0707–495 without changing T_{in} (Boller et al. 2003; Gallo et al. 2004). We therefore suspect that the observed flux variations are not all due to the luminosity changes of the central source.

The possibility of partial covering causing large flux changes in NLS1 was previously considered (Boller et al. 1997; Brandt & Gallagher 2000). Tanaka et al. (2003) demonstrated, from a study of a dip in the light curve of GRO J1655-40, that spectrum-invariant flux changes can occur as a result of changes in partial covering conditions. A similar condition is illustrated in figure 2 for the case of 1H 0707–495. The parameters of the MCD and of one partial coverer (f and N_{H}) are fixed to the best-fit values of the observed spectrum (Fe abundance of $3 \times$ solar assumed), and those of the second coverer (f_2 and $N_{\text{H},2}$) are varied. Among them, (a) is the intrinsic spectrum and (d) is the best fit to the observed spectrum. The spectral shapes of (b) through (f) are similar to each other over a flux range of an order of magnitude. Positive correlation between f_2 and $N_{\text{H},2}$ is plausible, as discussed in Tanaka et al. (2003).

The observed light curve of 1H 0707–495 (figure 3 of Paper 1) appears as consisting of random “flares” of various peak fluxes, each lasting typically $\sim 3 \cdot 10^3$ s. Such flux changes can be explained qualitatively as follows: If the azimuthal distribution of the covering clouds is non-uniform, the covering fraction varies according to the orbital motion of the clouds. A local minimum of the covering fraction corresponds to a flare peak.

The duration of a flare is the time that a local minimum of covering takes to scan the electron-scattering region from a distance r at the Keplerian velocity $c(r_g/r)^{1/2}$, where r_g is the gravitational radius. Suppose the electron-scattering region has an extension of $\sim 10r_g$, then the observed time scale is understood when these clouds are located around $r \sim 400r_g$ ($\sim 2 \cdot 10^{14}$ cm) for $M \sim 3 \cdot 10^6 M_\odot$.

The essential neutrality of iron indicates low photoionization effect, i.e. the ionization parameter $\xi = L_h/nr^2 \lesssim 1$, where L_h is the hard component luminosity and n the atomic density. This requires that $n \gtrsim 10^{14} \text{ cm}^{-3}$ for an estimated $L_h \sim 10^{43} \text{ erg s}^{-1}$. Such dense clouds are probably confined by magnetic fields (Rees 1987). In fact, the results from magneto-hydrodynamical simulations that demonstrate highly inhomogeneous and clumpy accretion flow are consistent with this view (e.g. Kawaguchi et al. 2000).

The persistent variation of the observed flux of 1H 0707–495 may be related to very high, possibly super-Eddington, luminosity (see subsection 3.2). At these accretion rates, various disk instabilities might produce inhomogeneities in the vertical direction, causing time-variable partial covering. An alternative possibility is that partial covering clouds may be formed from a radiation-driven mass outflow.

Large-amplitude variability is generally characteristic of NLS1. It is worth examining the associated spectral variation of other NLS1. If T_{in} of the soft component does not change with flux, it is possible that the flux variation may, at least in part, be due to changes in partial covering. If it were the case, the intrinsic luminosity, hence the black hole mass, could be significantly higher than estimated from the observed flux.

The authors are grateful to S. Mineshige for valuable comments.

References

- Abramowicz, M.A., Czerny, B., Lasota, J.P., & Szuszkiewicz, E. 1988, *ApJ* 332, 646
 Boller, Th., Brandt, W.N., Fabian, A.C., & Fink, H.H. 1997, *MNRAS* 289, 393
 Boller, Th. 2000, *New Astron. Rev.* 44, 387
 Boller, Th., et al. 2002, *MNRAS* 329, L1 (Paper 1)
 Boller, Th., Tanaka, Y., Fabian, A., Brandt, W.N., Gallo, L., Anabuki, N., Haba, Y., & Vaughan, S. 2003, *MNRAS* 343, L89
 Brandt, W.N., Fabian, A.C., Dotani, T., Nagase, F., Inoue, H., Kotani, T., & Segawa, Y. 1996, *MNRAS* 283, 1071

Brandt, W.N., Gallagher, & S.C. 2000, *New Astron. Rev.* 44, 461
Fabian, A.C., Ballantyne, D.R., Merloni, A., Vaughan, S., Iwasawa, K., & Boller, Th. 2002, *MNRAS* 331, L35
Gallo, L., Boller, Th., Tanaka, Y., Fabian, A.C., Brandt, W.N., Welsh, W. F., Anabuki, N. & Haba, Y. 2004, *MNRAS* 347, 269
Kawaguchi, T., Mineshige, S., Machida, M., Matsumoto, R., & Shibata, K. 2000, *PASJ* 52, L1
Makishima, K., et al. 2000, *ApJ* 535, 632
Mineshige, S., Kawaguchi, T., Takeuchi, M., & Hayashida, K. 2000, *PASJ* 52, 499
Mitsuda, K., et al. 1984, *PASJ* 36, 741
Pounds, K., Done, K., & Osborne, J.P. 1995, *MNRAS* 277, L5
Rees, M.J. 1987, *MNRAS* 228, 47p
Ross, R.R., Fabian, A.C., & Mineshige, S. 1992, *MNRAS* 258, 189
Tanaka, Y., & Shibazaki, N. 1996, *ARA&A* 34, 607
Tanaka, Y., Ueda, Y., & Boller, Th. 2003, *MNRAS* 338, L1
Watarai, K., Mizuno, T., & Mineshige, S. 2001, *ApJ* 549, L77